Hydrol. Earth Syst. Sci. Discuss., doi:10.5194/hess-2016-186, 2016
Manuscript under review for journal Hydrol. Earth Syst. Sci.
Published: 17 May 2016

Hydrology and Earth System Sciences
Open Access
Discussions

Examining the relationship between intermediate scale soil moisture and terrestrial evaporation within a semi-arid grassland

Raghavendra B. Jana, Ali Ershadi, and Matthew F. McCabe
Water Desalination and Reuse Centre, Division of Biological and Environmental Sciences and Engineering, King Abdullah University of Science and Technology, Thuwal 23955, Saudi Arabia.

Correspondence to: Raghavendra B. Jana (Raghavendra.Jana@kaust.edu.sa)

Abstract. Interactions between soil moisture and terrestrial evaporation affect water cycle behaviour and responses between the land surface and the atmosphere across scales. With strong heterogeneities at the land surface, the inherent spatial variability in soil moisture makes its representation via point-scale measurements challenging, resulting in scale-mismatch when compared to coarser-resolution satellite-based soil moisture or evaporation estimates. The Cosmic Ray Soil Moisture Observing System (COSMOS) was developed to address such issues in the measurement and representation of soil moisture at intermediate scales. Here we present an examination of the links observed between COSMOS soil moisture retrievals and evaporation estimates over a pasture in the semi-arid central-west region of New South Wales, Australia. The COSMOS soil moisture product was compared to evaporation derived from three distinct approaches, including the Priestley-Taylor (PT-JPL), Penman-Monteith (PM-Mu) and Surface Energy Balance System (SEBS) models, driven by forcing data from local meteorological station data and remote sensing retrievals from the Moderate Resolution Imaging Spectroradiometer (MODIS) sensor. Pearson's Correlations, Quantile-Quantile (Q-Q) plots, and Analysis of Variance (ANOVA) were used to qualitatively and quantitatively evaluate the temporal distributions of soil moisture and evaporation over the study site. The relationships were examined against nearly two years of observation data, as well as for different seasons and for defined periods of analysis. Results highlight that while direct correlations of raw data were not particularly instructive, the Q-Q plots and ANOVA illustrate that the root-zone soil moisture represented by the COSMOS measurements and the modelled evaporation estimates reflect similar distributions under most meteorological conditions. The PT-JPL and PM-Mu model estimates performed contrary to expectation when high soil moisture and cold temperatures were present, while SEBS model estimates displayed a disconnect from the soil moisture distribution in summers with long dry spells. Importantly, no single evaporation model matched the statistical distribution of the measured soil moisture for the entire period, highlighting the challenges in effectively capturing evaporative flux response within changing landscapes.

Keywords: *COSMOS; soil moisture; land surface evaporation; SEBS; PM-Mu; PT-JPL*

Hydrol. Earth Syst. Sci. Discuss., doi:10.5194/hess-2016-186, 2016
Manuscript under review for journal Hydrol. Earth Syst. Sci.
Published: 17 May 2016

1. Introduction

Land surface evaporation (referred to commonly as ET) and soil moisture play major roles in defining the water cycle behaviour of landscapes as well as controlling the feedback from the land surface to the atmosphere at various spatial and temporal scales (Manfreda et al. 2007; Seneviratne et al. 2010). Land surface evaporation, comprising the processes of plant transpiration, evaporation from the soil and evaporation from canopy intercepted rainfall, has been estimated to return almost 70% of precipitated water back to the atmosphere (Hanson 1991; Trenberth et al. 2011). In arid and semi-arid regions, this value can be much larger. Although coupling is expected to be high in such environments, surface-atmosphere feedback dynamics are commonly less understood in arid/semi-arid regions (Wang et al. 2012). Several studies have attempted to describe these links, with the aim of predicting one variable through knowledge of the other (Mintz and Walker 1993; Wetzel and Chang 1987) or to use developed relationships to inform upon linked hydrological responses such as evaporation (McCabe et al. 2005; Stisen et al. 2011), soil moisture (Liu et al. 2012), drought (Entekhabi et al. 1992; Fischer et al. 2007; Oglesby and Erickson 1989), precipitation (Findell et al. 2011; Held et al. 2005), and even vegetation response to soil moisture stress (Liu et al. 2011).

The coupling between soil moisture and the overlaying atmosphere has been a topic of intense investigation in recent years. Koster et al. (2006) compared multiple atmospheric general circulation models with regard to the strength of land-atmosphere couplings and reported that while the coupling strengths varied widely for the models, most models agreed upon certain locations of high land-atmosphere coupling. Dirmeyer (1994) used a simple biosphere model to evaluate the effect of soil moisture and vegetation stress on the climatology of drought, while Martens et al. (2016) presented that assimilating SMOS derived soil moisture improved model estimates of terrestrial evaporation at the continental scale. Land-atmosphere coupling studies have also investigated, among others aspects, the impact of soil moisture on precipitation (Eltahir 1998; Koster et al. 2004; Schär et al. 1999) and how this knowledge can be an indicator of climate change (Seneviratne et al. 2006); the links between soil moisture and cloud cover (Betts 2004); and also how the ENSO cycle influences the coupling and the surface-atmosphere feedbacks (Miralles et al. 2014). A common feature of such studies is the use of model estimates of terrestrial evaporation across a wide range of study areas and land cover and biome types. The reliance on these model estimates necessitates a more critical examination of both the models used and an evaluation of their performance.

The Global Energy and Water Cycle Exchanges (GEWEX) LandFlux project (McCabe et al. 2016) and the related Water Cycle Multi-mission Observation Strategy – Evapotranspiration (WACMOS-ET) project (Michel et al. 2016; Miralles et al. 2016) reflect ongoing efforts to develop strategies for the prediction of land surface fluxes at regional and global scales. As part of these efforts, studies were undertaken to compare the remote sensing derived evaporation products with tower-based measurements: a standard approach to flux evaluation (Ershadi et al. 2014). However, such comparisons can suffer from both spatial and temporal scale mismatches, making robust evaluations inherently challenging. Generally, the spatial footprint of satellite-based sensors is much larger than the fetch of an eddy covariance tower. While tower-based sensors routinely record information at intervals of between 15-30 minutes, many satellite observations used in hydrological studies are often only available at daily time scales. Questions on the suitability of comparing large scale gridded evaporation estimates to fine scale tower observations have been raised previously (McCabe et al. 2016) and remain largely unresolved. As such, identifying complimentary observation sources that can be used to improve upon the evaluation of a variety of hydrological processes is a much needed objective (McCabe et al. 2008).

Generally, soil moisture measurements are made using either in-situ devices that are ground-based or via air- and satellite-borne sensors. While in-situ measurements tend to represent a spatial scale of the order of centimetres, remotely sensed soil moisture products have resolutions on the order of several hundred meters (air borne) to tens of kilometres (satellite borne) (Vereecken et al. 2007). Unfortunately, field scale spatial variability of soil moisture is generally smoothed out in the large scale soil moisture estimates (Manfreda et al. 2007). Technically, a number of point-scale measurements can be collected and then spatially averaged over a domain. However, such an approach is infeasible for continuous monitoring over multiple fields. As such, there is a clear need for resolving field scale heterogeneity at scales that can be monitored from remotely observing platforms: or conversely, providing ground based observations that better reflect the scale of satellite systems.

Different spatial scaling approaches have been employed to obtain soil moisture values at multiple resolutions (Jana and Mohanty 2012; Jana et al. 2008; Vereecken et al. 2007). In recent years, the challenge of obtaining intermediate resolution (between point scale and satellite resolution) soil moisture has been addressed by the Cosmic Ray Soil Moisture Observing System (COSMOS) developed by Zreda et al. (2012). Based on determining the neutron density of cosmic rays, COSMOS is able to make measurements of soil moisture at spatial resolutions of a few hundred meters. The COSMOS footprint, with a radius of 300-400 m, is comparable to that of airborne remote sensors, while being ground-based and capable of continuously recording soil moisture over long periods of time. Moreover, the effective measurement depth of the COSMOS sensor ranges from 12 to 76 cm. This depth allows the sensor to capture the root zone soil moisture dynamics to a great extent (Desilets et al. 2010). Evaporation and transpiration processes are influenced significantly by the root zone soil moisture. Transpiration rates depend upon the amount of plant-available water in the root zone, while evaporation plays a regulatory role in governing the dynamics of the surface soil moisture. It is well recognized that soil moisture is a limiting factor in the evaporative process (Seneviratne et al. 2010), playing an important role in modulating plant stress and vegetation response. With improved sensing of the root-zone soil moisture, it is expected that any relationship between evaporation and soil moisture will be more robust.

Given these developments and outstanding challenges, the objective of this study is to investigate the potential of using COSMOS soil moisture retrievals to evaluate modeled evaporation estimates derived from a combination of tower based and remote sensing inputs. The capacity to indirectly monitor surface flux responses using such data offers a mechanism through which land-atmosphere couplings can be explored and provides an additional constraint on coupled water and energy cycle modeling at the land surface. In order to achieve this objective, we conducted an exploratory study that examined the link between the soil moisture retrievals from COSMOS and evaporation estimates collected over a semi-arid grassland. The underlying hypothesis to be tested here is that rainfall input in such landscapes will be well reflected by the soil moisture values, which in turn should be strongly coupled to evaporation.

2. Data and Methodology

2.1. Study area

The study was conducted at a pasture near Baldry, a rural township in New South Wales, Australia. The site is classified as a semi-arid region with latitude -32.87 degrees, longitude 148.52 degrees, and an elevation of 438 m above mean sea level. The Baldry experimental catchment formed part of the Australian National Cosmic Ray Soil Moisture Monitoring Facility (CosmOz) network, established by the Commonwealth Scientific and Industrial Research Organization (CSIRO) (Hawdon et al. 2014). A COSMOS probe was put in place at the site in March 2011, complimenting existing meteorological and soil moisture sensors, as well as an eddy-covariance flux tower. Figure 1 details the location of the Baldry test site. Further details regarding the instrumentation at the Baldry test site and the CosmOz network in general are provided by Hawdon et al. (2014) (see also http://cosmoz.csiro.au/sensor-information/?SiteNo=1).

2.2. Description of evaporation models

2.2.1 PT-JPL

Of the three evaporation models evaluated in this study, the Priestley-Taylor Jet Propulsion Laboratory (PT-JPL) model uses the least number of meteorological and remote sensing input data, including air temperature, humidity, net radiation and a vegetation index (Fisher et al. 2008). This model has been used to estimate actual evapotranspiration at local (Ershadi et al. 2014) and global scales in various studies (e.g., Badgley et al. 2015; Ershadi et al. 2014; Vinukollu et al. 2011) as well as the recent LandFlux (McCabe et al. 2016) and WACMOS-ET (Miralles et al. 2016) efforts. The PT-JPL is a three source model. The total evaporation is partitioned into soil evaporation (λE_s), canopy transpiration (λE_t), and wet canopy evaporation (λE_i), i.e. $\lambda E = \lambda E_s + \lambda E_t + \lambda E_i$. The model initially partitions the net radiation into soil and vegetation components and then estimates the potential evaporation from the three sources - soil, canopy and wet canopy. The effects of green cover fraction, relative wetness of the canopy, air temperature, plant water stress and soil water stress on the evaporative process are represented by corresponding multipliers which are subsequently determined. The actual evaporation values for each component of the system are then computed by reducing the potential evaporation based on these constraint multipliers. Further details of the PT-JPL model can be found in the article by Fisher et al. (2008).

2.2.2 PM-Mu

The Penman-Monteith based model developed by Mu et al. (2011) (PM-Mu) is another three-source scheme that has been used in a range of applications for estimating terrestrial fluxes (Mu et al. 2013), including forming the basis behind the global evaporation product (MOD16) (Mu et al. 2013). The PM-Mu model computes total evaporation as the sum of the three components: soil evaporation, canopy transpiration and evaporation of the intercepted water in the canopy, i.e. ($\lambda E = \lambda E_s + \lambda E_t + \lambda E_i$). While based on the Penman-Monteith equation (Monteith 1965), the evaporation from each component is estimated by assigning weights to the fractional vegetation cover, relative surface wetness and available energy. Plant phenology and climatological data are used to extend biome-specific conductance parameters from the stomata to the canopy scale. The extended conductance parameters are then used to parameterize aerodynamic and surface resistances for each component source. Further details regarding the PM-Mu model can be found in the publications by Mu et al. (2011) and Mu et al. (2013), along with recent evaluations studied from the local (Ershadi et al. 2014; Michel et al. 2016) to the global scales (McCabe et al. 2016; Miralles et al. 2016).

2.2.3 SEBS

The Surface Energy Balance System (SEBS) model (Su 2002) is a physically-based scheme that has been widely used in estimating evaporation across a range of scales (Elhag et al. 2011; McCabe and Wood 2006; Su et al. 2005). The model utilizes commonly available hydrometeorological variables, including net radiation, land surface temperature, air temperature, humidity, wind speed and vegetation phenology to calculate both latent and sensible heat surface fluxes. The model first calculates land surface roughness parameters, including roughness lengths for momentum and heat transfer using a method developed by Su et al. (2001). These roughness parameters are then applied to a set of flux-gradient equations along with temperature gradient and wind speed data to compute the sensible heat flux. The flux-gradient equations quantify the heat transfer between the land surface and the atmosphere. SEBS uses either the Monin-Obukhov Similarity Theory (MOST) or the Bulk Atmospheric Similarity Theory (BAST) equations (Brutsaert 2005), based on the height of the atmospheric boundary layer. SEBS then determines the sensible heat flux under hypothetical extreme wet and dry conditions to calculate the evaporative fraction. Latent heat flux is estimated as a component of the available energy based on the calculated evaporative fraction. Further details regarding the SEBS model and its formulation can be found in the work of Su (2002).

2.3. Datasets

Following is a brief review of the data that has been used in the analysis, as well as a description of the standardization process employed to allow comparison of these distinct datasets.

2.3.1 Eddy-covariance surface fluxes

An eddy covariance system provided measurement of heat fluxes and radiation components for periods throughout the duration of the COSMOS installation. The system comprised of a Campbell Scientific 3D sonic anemometer (CSAT-3, Campbell Scientific, Logan, UT, USA) along with a LiCOR 7500 (Li-7500, LiCor Biosciences, Lincoln, NB, USA) for high-frequency water vapor and CO2 concentrations. Turbulent flux data was sampled at 10 Hz, with flux values averaged to 30 minute intervals. A meteorological tower was co-located alongside the eddy covariance system, with a Kipp and Zonen CNR4 radiometer, Apogee infrared surface temperature, RIMCO rain gauge, Vaisala HMP75C temperature and humidity probe, RM Young wind sentry (wind speed and direction), Huskeflux ground heat flux plate and Vaisala BaroCap barometric pressure sensor. Both tower meteorological and eddy-covariance data were quality controlled to detect and remove errors. The low-frequency 30 minute resolution data were corrected for coordinate rotation (Finnigan et al. 2003) and WPL effects (Leuning 2007) using the PyQC software tool (available from code.google.com/p/eddy). These data were then accumulated to form 24-hourly totals for each day of the available observation period.

2.3.2 Satellite-based observations

Information required for the different evaporation models (see Section 2.2) were obtained using both the tower-based observations as well as the Moderate-Resolution Imaging Spectroradiometer (MODIS) sensor on board NASA's Terra and Aqua satellites. Land surface temperature data required for the SEBS model were derived from the daily MOD11A1 and MYD11A1 products of the Terra and Aqua satellites (Wan 2009). Normalized Difference Vegetation Index (NDVI) data (used by all models) were obtained from the MOD13Q1 product (Solano et al. 2010).

2.3.3 Soil Moisture

The intermediate scale soil moisture data used in this study was obtained from the COSMOS repository (http://cosmos.hwr.arizona.edu/Probes/StationDat/078/). The COSMOS device was active at the Baldry site for the period March 30, 2011 to March 13, 2014. Accounting for gaps in the dataset due to instrument outage as well as the availability of concurrent ancillary data such as the remote sensing inputs required for the evaporation models, a total of 684 days from 2011-2013 were selected for the study. The 15-minute temporal frequency of COSMOS soil moisture estimates were averaged to the daily time scale. In addition to the COSMOS data, soil moisture observations from three water content reflectometers (CS616, Campbell Scientific, Logan, UT, USA) installed at the site were also used. The TDR sensors had probe lengths of 30 cm length that were inserted vertically from the surface at three locations around the COSMOS instrument. An average of the three TDR measurements was computed at each time step for comparison with the COSMOS soil moisture estimates.

2.4. Data Standardization

Volumetric soil moisture obtained via the COSMOS probe is reported in units of $cm^3.cm^{-3}$ and represents a fraction that is always less than a theoretical maximum of 1. Evaporation estimates are represented in units of mm and have a less defined theoretical upper bound. In order to compare these quantities across different units and ranges, evaporation and soil moisture data were standardized by computing the standard score, i.e.,

$$X_{st} = \frac{X - \bar{X}}{\sigma} \quad (1)$$

where X_{st} is the standardized data point, X is the raw data, $\bar{X}$ is the mean of the raw dataset, and σ is the standard deviation of the raw dataset. Reducing data with different units to units of standard deviation helps to compare the distributions of dissimilar quantities. Standardizing raw data before comparison of distributions with different means and scales of variation is a common practice (Koster et al. 2011; Zhang et al. 2008). Importantly, doing so does not change the statistical analyses, as the data are simply scaled to be comparable to each other.

3. Analyses and Discussion

3.1. Correlation of COSMOS soil moisture and evaporation at the EC tower

Given that modelled evaporation estimates are generally validated against observations from eddy covariance towers (Ershadi et al. 2014), an initial step in our study was to query the relationship between the COSMOS soil moisture retrieval and the tower-based evaporation observations. Figure 2a shows a scatter of the raw (non-standardized) COSMOS soil moisture daily averages plotted against the corresponding 24-hour daily evaporation values observed at the eddy covariance tower on site. The two quantities have a Pearson's correlation coefficient close to 0.40. Figure 2b shows the scatter of change in soil moisture on a daily scale versus the corresponding change in observed evaporation across a daily interval for the entire period of record at the Baldry site. The plot is clustered around the zero change values, with a correlation coefficient of -0.26. These low correlations suggest that the COSMOS soil moisture and the observed evaporation are statistically not well correlated with each other. However, comparing the cumulative distribution (CDF) of the change in soil moisture state at each daily time step to the CDF of the corresponding change in observed evaporation (Figure 2d) demonstrates a visible similarity between the two quantities. Physically, it makes sense that the change in evaporation should be correlated to change in soil moisture, even if the raw data are not. This relationship is brought out at the distribution level, while the point-to-point comparison fails to do so. The CDF's of the raw data (Figure 2c) also show that the quantities behave similar to each other, albeit with a shift in scale. Soil moisture and land surface evaporation are both processes with inherent stochasticity in their determination, due in part to the imprecise nature of physical measurement i.e. field-based observations of these processes are inferred rather than measured in an absolute sense. In such situations, it is often more appropriate to analyse the quantities for their similarity of statistical distributions rather than deducing a lack (or presence) of a relationship based on point-to-point statistics such as correlation.

3.2. Analyses of standardized data distributions

Figure 3 shows the precipitation data at the study site, together with the standardized COSMOS soil moisture and evaporation estimates from the PT-JPL, PM-Mu and SEBS models. The average TDR soil moisture measurements, and the evaporation observed from the in-situ eddy covariance tower, are also shown. As can be seen, the COSMOS and TDR soil moisture series reflect similar responses in their variability and seasonality, with the COSMOS data indicating greater fine-scale variability. While it might be expected that the TDR data should display greater variability in response, the COSMOS measurements have higher variability in soil moisture values, perhaps due to its greater penetration depth into the soil profile and larger spatial extent.

With the aim of investigating the link between the COSMOS soil moisture and the modeled evaporative response, non-parametric quantile-quantile (Q-Q) plots and box plots were used. Figure 4 shows the Q-Q plots for the standardized soil moisture data versus the standardized model derived evaporation estimates. The inter-quartile range is highlighted in grey and the red line denotes the extrapolation of the slope of the inter-quartile range. Good agreement between the Q-Q plot and the

Hydrol. Earth Syst. Sci. Discuss., doi:10.5194/hess-2016-186, 2016
Manuscript under review for journal Hydrol. Earth Syst. Sci.
Published: 17 May 2016

red expectation line indicates that the two quantities have been sampled from the same distribution. It can be seen that for all three models, the evaporation and soil moisture relationships follow the expectation (red line) closely, particularly in the inter-quartile range. This indicates that the two independent datasets (modelled evaporation and COSMOS soil moisture) are sampled from distributions that are very similar to each other. However, beyond the inter-quartile range, a deviation of the plot away from the expectation line is seen in all cases. This is more apparent at the extremes. The SEBS estimates deviate more from the expectation on the higher side of the inter-quartile range, as compared to the other two models. However, this behaviour is similar to that of the measured evaporation from the eddy covariance tower, as can be seen from the last plot in Figure 4. Towards the higher end of the data range, the PT-JPL and PM-Mu values, while close to the expectation, are underestimated when compared to the tower measurements.

The above observation is additionally supported by the boxplots resulting from the one-way Analysis of Variance (ANOVA) test, which are shown in Figure 5. In general, an ANOVA test generates a box plot along with a table of statistics, the most important of which is typically the p-value. The p-value, ranging between 0 and 1, signifies how dissimilar the average values of two datasets are from each other. A high p-value signifies that the two averages are statistically similar to each other, and vice versa. However, for this study, the datasets were standardized to have zero-mean distributions in order to enable comparison between quantities having different units and ranges. Hence, in this case, the ANOVA test would always return a p-value of 1, indicating that the two means are statistically identical. The p-value is, therefore, not suitable to understand the behaviour of the two datasets. Hence, the ANOVA boxplots are preferred in this case as they provide insight into the distribution-level behaviour of the datasets.

From Figure 5 it can be seen that the COSMOS soil moisture distribution is slightly skewed to the left (shorter tail below the first quartile), while the evaporation model estimates are more symmetrically distributed. Again, as in the Q-Q plots, the inter-quartile ranges are very similar for both hydrological variables. In this case, the SEBS evaporation estimates have more outliers on the higher side, as compared to the other two model estimates.

3.3. Analysis of relationship based on defined periods

In order to get a better understanding of the observed dynamics between the soil moisture and evaporation signatures, we divided the data time series into four distinct sub-periods based on short-term trends and the level of correspondence between the soil moisture and evaporation records. Period 1 ran from day of record (DoR) 55 to 144. In the course of this period both the soil moisture and the modelled evaporation had a steady descending tendency (see Figure 3). The soil moisture and evaporation signatures behaved consistent with each other in both increasing and decreasing tendencies during Period 2, running from DoR 321 to 410. Period 3, between DoR 410 and DoR 500, covers a series of wetting and drying cycles of soil moisture, while no such corresponding changes were observed in the evaporation signatures. Period 4, covering the period between DoR 501 and DoR 590, exhibits signatures that oppose each other in behaviour such that an increase in soil moisture corresponds to a decrease in the estimated evaporation. The four sub-periods were selected to examine the relationship between the COSMOS soil moisture and the model derived evaporation estimates under diverse hydrological conditions. Data from these sub- periods were individually standardized using the mean and standard deviation for each particular period.

Q-Q plots of COSMOS soil moisture against the model-derived evaporation estimates for each of the four sub-periods are shown in Figure 6. The corresponding Pearson's correlation value (R) for each of the modelled evaporation estimates with regard to the COSMOS soil moisture is also included. In these analyses, the R-value is used to assess the relative performance of the models during each specific period, and not as an absolute indicator. During sub-periods 1 and 2, the Q-Q plots indicate that the soil moisture and evaporation model-estimates were both sampled from similar distributions, particularly in the inter-quartile range (IQR). Quantile values of the standardized PT-JPL model estimates have the closest match with the soil moisture values during Period 1, both within and outside the IQR. This observation is supported by the PT-JPL estimate having a higher correlation (0.108) with the soil moisture among the three model estimates. During Period 2, the PM-Mu model estimates display a higher correlation (0.764) with the soil moisture than any of the other two models. However, if we limit the analysis to the IQR data, where the bulk of the data resides, the SEBS model (R=0.714) has a closer match to the expectation line. For Period 3, a simple visual analysis of the standardized time series of soil moisture and evaporation would indicate that the two quantities were probably de-coupled. However, the Q-Q plots for this period display that there is substantial correspondence between the two datasets. This demonstrates that although the changes in the evaporation were small when compared with the soil moisture variability for this period, evaporation was still being driven by the root zone soil moisture. Also, while the scales are shifted, the Q-Q plots suggest that the evaporation values are still being sampled from a distribution similar to that of the soil moisture. The PT-JPL model estimates track the expectation line closely within the IQR, and on the higher extremes beyond the IQR. Below the IQR, all three models behave consistently with each other, suggesting that as the soil gets drier, the three models studied here all converge towards similar estimates of evaporation. During this period, negative correlations with the soil moisture are observed for all three model ET estimates.

The Q-Q plots for sub-period 4 show that there is a marked incongruity between the distributions of soil moisture and the PT-JPL evaporation estimates. The plot deviates from the line representing the slope of the IQR, particularly within IQR where the bulk of the data would be expected to lie. This behaviour indicates that during this sub-period, the modelled evaporation was de-coupled from the soil moisture signature. The other three-source model (PM-Mu), also exhibits this de-coupling, although to a lesser extent. However, the de-coupling is not seen in the flux estimates of the SEBS model. The PT-JPL and PM-Mu estimates also show negative correlation with the soil moisture during this period, while the SEBS estimate is positively correlated. Period 4, corresponding with the Australian winter (May-July 2012), received frequent rainfall events (Figure 3) that resulted in elevated soil moisture levels while the cloud cover probably limited the energy available for the evaporation process.

Comparisons between the ANOVA boxplots of the model-derived evaporation to the COSMOS soil moisture and the observed flux from the eddy covariance tower, for each period of the trends-based analysis, are shown in Figure 7. During Period 4, the modelled evaporation distributions are significantly different from the eddy-covariance measured at the tower, especially for the PT-JPL and PM-Mu models. The observed evaporation has a distribution that is closer to that of the COSMOS soil

Hydrol. Earth Syst. Sci. Discuss., doi:10.5194/hess-2016-186, 2016
Manuscript under review for journal Hydrol. Earth Syst. Sci.
Published: 17 May 2016

moisture, while the distributions of the PT-JPL and PM-Mu estimates are skewed to the left. The PT-JPL and PM-Mu methods are based primarily on the available energy (Rn-G) of the system, with soil moisture being implicitly accounted for by adjusting the air humidity. The Penman (1948) and Penman-Monteith (Monteith 1965) combination equations that form the theoretical basis for the PT-JPL and PM-Mu models, were developed for and tested (Rana and Katerji 1998; Shahrokhnia and Sepaskhah 2011; Sumner and Jacobs 2005) in situations where energy limitations were not present. In contrast, the SEBS model follows a more physically-based approach dependent on the turbulent mixing theory (Brutsaert 2013), which is valid in energy-limited situations similar to those observed during Period 4. It is also likely that low temperatures and additional hydro-meteorological factors could have caused a de-coupling of the soil moisture from the air humidity. In such a scenario, regardless of the presence of abundant soil moisture for evaporation, the models may report lower estimates compared to those observed from the eddy-covariance tower. These factors may represent physical constraints on the application of the PT-JPL and PM-Mu methods and require further investigation.

3.4. Analysis of the relationship based on seasonal behaviour

To understand the seasonal patterns in the relationship between the COSMOS soil moisture and the evaporation data, the two-year record of data was partitioned according to seasons. The period between December and February corresponds to the Austral summer, while autumn is from March to May, winter from June to August, and spring from September to November. The summer and spring seasons experienced the greatest number of precipitation events (defined here as rainfall greater than 1 mm/day) with 34 and 33 rainy days out of a total of 164 and 181 days of records respectively, followed by winter (26 events in 184 days) and autumn (17 events in 155 days).

Corresponding Q-Q plots for the four seasons are shown in Figure 8. In the autumn, the PM-Mu evaporation estimates correspond most closely with the COSMOS soil moisture retrievals in the inter-quartile range (IQR), followed by the SEBS estimates. PT-JPL performed the poorest. Beyond the IQR, and overall, the SEBS estimates were the closest match to the soil moisture distribution in this season. In winter, the PT-JPL estimates were the closest to the soil moisture distribution within the IQR, while overall the SEBS model again performed best, relative to these specific metrics. In the spring, the SEBS model estimates were distributed most similar to the soil moisture, both within the IQR and overall. PM-Mu estimates were the least similarly distributed.

The summer season shows that all three evaporation estimates depart from the expectation within the IQR, with the SEBS estimates being least similar and the PT-JPL estimates most similar to the soil moisture distribution. As mentioned above, the site experienced 34 rainfall events out of a total of 164 days of record. However, there were also long periods with no rainfall events. Combined with the higher temperatures of summer, this leads to greater non-monotonic variations in the soil moisture signature, thus creating a disconnect with the evaporation patterns. It has been demonstrated previously that the occurrence of hot and dry periods leads to decoupling of soil moisture and evaporation (Pollacco and Mohanty 2012). The soil moisture profile in such situations becomes heterogeneous. Evaporation variability in summer is driven more by the precipitation patterns than the soil moisture. With an abundance of energy, and severe limitation of soil moisture, any influx of moisture due to precipitation is quickly evaporated back to the atmosphere. Despite this, in an example of the "correlation does not imply causation" maxim, it is observed that the evaporation estimates for this season exhibit the highest correlation (R-value) with the COSMOS soil moisture. High soil moisture and temperature conditions in summer could also increase uncertainty in the surface-to-air temperature gradient: a key element of the SEBS approach. The SEBS model has been shown to be highly sensitive to the temperature gradient parameterization (Ershadi et al. 2013), and this might be a reason for its poor performance in the summer period.

From Figure 8, it is also seen that in most cases, the PT-JPL and PM-Mu models underestimate the evaporation at the higher end of the scale, at least when compared with the eddy-covariance tower measurements. The SEBS model generally performs better in this regard, as also seen in the previous analysis of the shorter time series (Figure 5). Previous studies have shown that SEBS based evaporation estimates were found to correspond well with tower-based measurements when there is a short, homogeneous canopy (McCabe et al. 2016) and the Baldry grassland site meets this criterion.

3.5. Caveats, limitations and suggestions for future direction

Correlation analyses are based on one-to-one comparison between datasets. Q-Q plots, on the other hand are a measure of the similarity of distribution. While there may be low point-to-point correlation between two datasets, it is very much possible that the two quantities are sampled from the same (or similar) distributions (Jana et al. 2008). Such correspondence at the distribution level, rather than at the point level, is much more meaningful for stochastic variables such as soil moisture and ET. Hence, we emphasize the agreement in the Q-Q plots rather than the R value in our study. Other potential causes of errors could be uncertainties in the observed data from the COSMOS instrument and the eddy-covariance, cloud cover resulting in inaccurate MODIS observations which could further lead to inconsistencies in the model outputs. Aditionally, uncertainties in the meteorological forcings and other model inputs have not been explored in this study. The model structure and variations in model parameterization could also affect the analyses. We have used the structure and parameterization described by Ershadi et al. (2014) as they have been shown to correspond well with the tower observations. Other model parameterizations may improve (or degrade) the correspondence with the soil moisture, but that investigation is beyond the scope of this preliminary study.

This study shows that intermediate resolution soil moisture can be used to validate and constrain models for land surface evaporation. Importantly, the soil moisture distribution can act as a guide for validating the model evaporation estimates in cases where eddy covariance data is either unavailable or of poor quality. Further, considering that the footprint of the tower observations is at a much finer scale in comparison with the gridded model estimates of evaporation, it may be more prudent to evaluate evaporation models using the COSMOS soil moisture, which is at a comparable resolution. Obviously, further analyses across different biomes and hydroclimatic regimes is necessary before a robust relationship between the model evaporation estimates and the COSMOS soil moisture can be established. However, the outcome of this study encourages such an effort to be made. As shown in earlier studies to validate gridded evaporation products (Ershadi et al. 2014; McCabe et al. 2016) no single evaporation model consistently performed better than others across all conditions, whether that was seasonal or based upon climate or biome-type. This suggests that an ensemble modelling approach with model weights assigned according to, among other factors, their established relationship with soil moisture may be more suitable.

4. Conclusions

Relationships between soil moisture observations from a COSMOS probe and evaporation estimates derived from three distinct model structures using a combination of tower and satellite-based data were examined across a semi-arid grassland site. Standardized daily evaporation and COSMOS soil moisture data were compared, with an analysis performed over different hydrological regimes, as well as an examination of seasonal scale variations. As theorised, the two hydrological variables displayed significant correspondence with each other over the entire time series, indicating that there is a solid connection relating them. It was also established that a relationship exists between the intermediate scale soil moisture measurements and the modelled evaporation estimates across most of the defined analysis periods. It was observed that the PT-JPL and PM-Mu model estimates behaved contrary to expectation in conditions where high soil moisture existed with colder temperatures. SEBS model estimates presented a similar disconnect from the soil moisture distribution, but in the summer season during long dry spells. These deviations are attributed to the model structures and reflect previous works identifying the geographic and temporal variability of model performance. Overall, no single model estimate of evaporation fully reproduced the COSMOS soil moisture across all conditions. However, the outcome of this study indicates that the intermediate scale soil moisture could be employed as a useful constraint to validate gridded evaporation estimates derived from models.

5. Acknowledgements

Research reported in this publication was supported by the King Abdullah University of Science and Technology (KAUST), Saudi Arabia. The COSMOS instrument was supported by the Commonwealth Scientific and Industry Research Organization (CSIRO). Instrumentation at the Baldry site was funded and commissioned as part of the Australian government's National Collaborative Research Infrastructure Strategy (NCRIS) and the University of New South Wales. Dr Ershadi was supported by the Australian Research Council Discovery Project (DP120104718).

References

Badgley, G., Fisher, J.B., Jimenez, C., Tu, K.P., & Vinukollu, R. (2015). On Uncertainty in Global Terrestrial Evapotranspiration Estimates from Choice of Input Forcing Datasets. *Journal of Hydrometeorology*, *16*, 1449-1455

Betts, A.K. (2004). Understanding Hydrometeorology Using Global Models. *Bulletin of the American Meteorological Society*, *85*, 1673-1688

Brutsaert, W. (2005). *Hydrology : An Introduction*. Cambridge: Cambridge University Press

Brutsaert, W. (2013). *Evaporation into the atmosphere: theory, history and applications*. Springer Science & Business Media

Desilets, D., Zreda, M., & Ferre, T.P.A. (2010). Nature's neutron probe: Land surface hydrology at an elusive scale with cosmic rays. *Water Resources Research, 46*

Dirmeyer, P.A. (1994). Vegetation stress as a feedback mechanism in midlatitude drought. *J. Climate, 7*, 1463-1483

Elhag, M., Psilovikos, A., Manakos, I., & Perakis, K. (2011). Application of the SEBS water balance model in estimating daily evapotranspiration and evaporative fraction from remote sensing data over the Nile Delta. *Water Resources Management, 25*, 2731-2742

Eltahir, E.A.B. (1998). A Soil Moisture–Rainfall Feedback Mechanism: 1. Theory and observations. *Water Resources Research, 34*, 765-776

Entekhabi, D., Rodriguez-Iturbe, I., & Bras, R.L. (1992). Variability in Large-Scale Water Balance with Land Surface-Atmosphere Interaction. *Journal of Climate, 5*, 798-813

Ershadi, A., McCabe, M., Evans, J., Chaney, N., & Wood, E. (2014). Multi-site evaluation of terrestrial evaporation models using FLUXNET data. *Agricultural and Forest Meteorology, 187*, 46-61

Ershadi, A., McCabe, M.F., Evans, J.P., Mariethoz, G., & Kavetski, D. (2013). A Bayesian analysis of sensible heat flux estimation: Quantifying uncertainty in meteorological forcing to improve model prediction. *Water Resources Research, 49*, 2343-2358

Findell, K.L., Gentine, P., Lintner, B.R., & Kerr, C. (2011). Probability of afternoon precipitation in eastern United States and Mexico enhanced by high evaporation. *Nature Geosci, 4*, 434-439

Finnigan, J.J., Clement, R., Malhi, Y., Leuning, R., & Cleugh, H.A. (2003). A Re-Evaluation of Long-Term Flux Measurement Techniques Part I: Averaging and Coordinate Rotation. *Boundary-Layer Meteorology, 107*, 1-48

Fischer, E.M., Seneviratne, S.I., Lüthi, D., & Schär, C. (2007). Contribution of land-atmosphere coupling to recent European summer heat waves. *Geophysical Research Letters, 34*, n/a-n/a

Fisher, J.B., Tu, K.P., & Baldocchi, D.D. (2008). Global estimates of the land-atmosphere water flux based on monthly AVHRR and ISLSCP-II data, validated at 16 FLUXNET sites. *Remote Sensing of Environment, 112*, 901-919

Hanson, R.L. (1991). Evapotranspiration and Droughts. In R.W. Paulson, E.B. Chase, R.S. Roberts, & D.W. Moody (Eds.), *National Water Summary 1988-89--Hydrologic Events and Floods and Droughts: U.S. Geological Survey Water-Supply Paper* (pp. 99-104)

Hawdon, A., McJannet, D., & Wallace, J. (2014). Calibration and correction procedures for cosmic-ray neutron soil moisture probes located across Australia. *Water Resources Research, 50*, 5029-5043

Held, I.M., Delworth, T.L., Lu, J., Findell, K.L., & Knutson, T.R. (2005). Simulation of Sahel drought in the 20th and 21st centuries. *Proceedings of the National Academy of Sciences of the United States of America, 102*, 17891-17896

Jana, R.B., & Mohanty, B.P. (2012). A topography-based scaling algorithm for soil hydraulic parameters at hillslope scales: Field testing. *Water Resources Research, 48*

Jana, R.B., Mohanty, B.P., & Springer, E.P. (2008). Multiscale Bayesian neural networks for soil water content estimation. *Water Resources Research, 44*

Koster, R.D., Dirmeyer, P.A., Guo, Z., Bonan, G., Chan, E., Cox, P., Gordon, C., Kanae, S., Kowalczyk, E., & Lawrence, D. (2004). Regions of strong coupling between soil moisture and precipitation. *Science, 305*, 1138-1140

Koster, R.D., Mahanama, S.P.P., Yamada, T.J., Balsamo, G., Berg, A.A., Boisserie, M., Dirmeyer, P.A., Doblas-Reyes, F.J., Drewitt, G., Gordon, C.T., Guo, Z., Jeong, J.H., Lee, W.S., Li, Z., Luo, L., Malyshev, S., Merryfield, W.J., Seneviratne, S.I., Stanelle, T., van den Hurk, B.J.J.M., Vitart, F., & Wood, E.F. (2011). The Second Phase of the Global Land–Atmosphere Coupling Experiment: Soil Moisture Contributions to Subseasonal Forecast Skill. *Journal of Hydrometeorology, 12*, 805-822

Koster, R.D., Sud, Y.C., Guo, Z., Dirmeyer, P.A., Bonan, G., Oleson, K.W., Chan, E., Verseghy, D., Cox, P., Davies, H., Kowalczyk, E., Gordon, C.T., Kanae, S., Lawrence, D., Liu, P., Mocko, D., Lu, C.-H., Mitchell, K., Malyshev, S., McAvaney, B., Oki, T., Yamada, T., Pitman, A., Taylor, C.M., Vasic, R., & Xue, Y. (2006). GLACE: The Global Land–Atmosphere Coupling Experiment. Part I: Overview. *Journal of Hydrometeorology, 7*, 590-610

Leuning, R. (2007). The correct form of the Webb, Pearman and Leuning equation for eddy fluxes of trace gases in steady and non-steady state, horizontally homogeneous flows. *Boundary-Layer Meteorology, 123*, 263-267

Liu, Y.Y., de Jeu, R.A.M., McCabe, M.F., Evans, J.P., & van Dijk, A.I.J.M. (2011). Global long-term passive microwave satellite-based retrievals of vegetation optical depth. *Geophys. Res. Lett., 38*, L18402

Liu, Y.Y., Dorigo, W.A., Parinussa, R.M., De Jeu, R.A.M., Wagner, W., McCabe, M.F., Evans, J.P., & Van Dijk, A.I.J.M. (2012). Trend-preserving blending of passive and active microwave soil moisture retrievals. *Remote Sensing of Environment, 123*, 280-297

Manfreda, S., McCabe, M.F., Fiorentino, M., Rodríguez-Iturbe, I., & Wood, E.F. (2007). Scaling characteristics of spatial patterns of soil moisture from distributed modelling. *Advances in Water Resources, 30*, 2145-2150

Martens, B., Miralles, D., Lievens, H., Fernández-Prieto, D., & Verhoest, N. (2016). Improving Terrestrial Evaporation Estimates over Continental Australia Through Assimilation of SMOS Soil Moisture. *International Journal of Applied Earth Observation and Geoinformation*

McCabe, M.F., Ershadi, A., Jimenez, C., Miralles, D.G., Michel, D., & Wood, E.F. (2016). The GEWEX LandFlux project: evaluation of model evaporation using tower-based and globally-gridded forcing data. *Geosci. Model Dev., 9*, 283-305

McCabe, M.F., Kalma, J.D., & Franks, S.W. (2005). Spatial and temporal patterns of land surface fluxes from remotely sensed surface temperatures within an uncertainty modelling framework. *Hydrology and Earth System Sciences, 9*, 467-480

McCabe, M.F., & Wood, E.F. (2006). Scale influences on the remote estimation of evapotranspiration using multiple satellite sensors. *Remote Sensing of Environment, 105*, 271-285

Michel, D., Jiménez, C., Miralles, D.G., Jung, M., Hirschi, M., Ershadi, A., Martens, B., McCabe, M.F., Fisher, J.B., Mu, Q., Seneviratne, S.I., Wood, E.F., & Fernández-Prieto, D. (2016). The WACMOS-ET project – Part 1: Tower-scale evaluation of four remote sensing-based evapotranspiration algorithms. *Hydrol. Earth Syst. Sci., 20*, 803-822

Mintz, Y., & Walker, G. (1993). Global fields of soil moisture and land surface evapotranspiration derived from observed precipitation and surface air temperature. *Journal of Applied Meteorology, 32*, 1305-1334

Miralles, D.G., Jiménez, C., Jung, M., Michel, D., Ershadi, A., McCabe, M.F., Hirschi, M., Dolman, A.J., Fisher, J.B., Martens, B., Mu, Q., Seneviratne, S.I., Weber, U., Wood, E.F., & Fernández-Prieto, D. (2016). The WACMOS-ET project – Part 2: Evaluation of global land evaporation data sets. *Hydrol. Earth Syst. Sci., 20*, 823-842

Miralles, D.G., van den Berg, M.J., Gash, J.H., Parinussa, R.M., de Jeu, R.A.M., Beck, H.E., Holmes, T.R.H., Jiménez, C., Verhoest, N.E.C., Dorigo, W.A., Teuling, A.J., & Johannes Dolman, A. (2014). El Niño–La Niña cycle and recent trends in continental evaporation. *Nature Clim. Change, 4*, 122-126

Monteith, J.L. (1965). Evaporation and environment. *Symp. Soc. Exp. Biol., 19*, 205-234

Mu, Q., Zhao, M., Kimball, J.S., McDowell, N.G., & Running, S.W. (2013). A Remotely Sensed Global Terrestrial Drought Severity Index. *Bulletin of the American Meteorological Society, 94*, 83-98

Mu, Q., Zhao, M., & Running, S.W. (2011). Improvements to a MODIS global terrestrial evapotranspiration algorithm. *Remote Sensing of Environment, 115*, 1781-1800

Oglesby, R.J., & Erickson, D.J. (1989). Soil Moisture and the Persistence of North American Drought. *Journal of Climate, 2*, 1362-1380

Penman, H.L. (1948). Natural Evaporation from Open Water, Bare Soil and Grass. *Proceedings of the Royal Society of London. Series A. Mathematical and Physical Sciences, 193*, 120-145

Pollacco, J.A.P., & Mohanty, B.P. (2012). Uncertainties of Water Fluxes in Soil–Vegetation–Atmosphere Transfer Models: Inverting Surface Soil Moisture and Evapotranspiration Retrieved from Remote Sensing. *Vadose Zone Journal, 11*

Rana, G., & Katerji, N. (1998). A Measurement Based Sensitivity Analysis of the Penman-Monteith Actual Evapotranspiration Model for Crops of Different Height and in Contrasting Water Status. *Theoretical and Applied Climatology, 60*, 141-149

Schär, C., Lüthi, D., Beyerle, U., & Heise, E. (1999). The Soil–Precipitation Feedback: A Process Study with a Regional Climate Model. *Journal of Climate, 12*, 722-741

Seneviratne, S.I., Corti, T., Davin, E.L., Hirschi, M., Jaeger, E.B., Lehner, I., Orlowsky, B., & Teuling, A.J. (2010). Investigating soil moisture–climate interactions in a changing climate: A review. *Earth-Science Reviews, 99*, 125-161

Seneviratne, S.I., Luthi, D., Litschi, M., & Schar, C. (2006). Land-atmosphere coupling and climate change in Europe. *Nature, 443*, 205-209

Shahrokhnia, M.H., & Sepaskhah, A.R. (2011). Evaluation of wheat and maize evapotranspiration determination by direct use of the Penman–Monteith equation in a semi-arid region. *Archives of Agronomy and Soil Science, 58*, 1283-1302

Solano, R., Didan, K., Jacobson, A., & Huete, A. (2010). MODIS Vegetation Index User's Guide. In: Vegetation Index and Phenology Lab, The University of Arizona

Stisen, S., McCabe, M.F., Refsgaard, J.C., Lerer, S., & Butts, M.B. (2011). Model parameter analysis using remotely sensed pattern information in a multi-constraint framework. *Journal of Hydrology, 409*, 337-349

Su, H., McCabe, M.F., Wood, E.F., Su, Z., & Prueger, J. (2005). Modeling evapotranspiration during SMACEX: Comparing two approaches for local-and regional-scale prediction. *J. Hydrometeorol., 6*, 910-922

Su, Z. (2002). The Surface Energy Balance System (SEBS) for estimation of turbulent heat fluxes. *Hydrology and Earth System Sciences Discussions, 6*, 85-100

Su, Z., Schmugge, T., Kustas, W.P., & Massman, W.J. (2001). An Evaluation of Two Models for Estimation of the Roughness Height for Heat Transfer between the Land Surface and the Atmosphere. *Journal of Applied Meteorology, 40*, 1933-1951

Sumner, D.M., & Jacobs, J.M. (2005). Utility of Penman–Monteith, Priestley–Taylor, reference evapotranspiration, and pan evaporation methods to estimate pasture evapotranspiration. *Journal of Hydrology, 308*, 81-104

Trenberth, K.E., Fasullo, J.T., & Mackaro, J. (2011). Atmospheric Moisture Transports from Ocean to Land and Global Energy Flows in Reanalyses. *Journal of Climate, 24*, 4907-4924

Vereecken, H., Kasteel, R., Vanderborght, J., & Harter, T. (2007). Upscaling Hydraulic Properties and Soil Water Flow Processes in Heterogeneous Soils. *Vadose Zone Journal, 6*

Vinukollu, R.K., Sheffield, J., Wood, E.F., Bosilovich, M.G., & Mocko, D. (2011). Multimodel Analysis of Energy and Water Fluxes: Intercomparisons between Operational Analyses, a Land Surface Model, and Remote Sensing. *Journal of Hydrometeorology, 13,* 3-26

Wan, Z. (2009). MODIS Land-Surface Temperature Algorithm Theoretical Basic Document (LST ATBD) - Version 3.3. In: ICESS, University of Clifornia, Santa Barbara

Wang, L., D'Odorico, P., Evans, J.P., Eldridge, D.J., McCabe, M.F., Caylor, K.K., & King, E.G. (2012). Dryland ecohydrology and climate change: Critical issues and technical advances. *Hydrology and Earth System Sciences, 16*, 2585-2603

Wetzel, P.J., & Chang, J.-T. (1987). Concerning the relationship between evapotranspiration and soil moisture. *Journal of climate and applied meteorology, 26*, 18-27

Zhang, J., Wang, W.C., & Wei, J. (2008). Assessing land-atmosphere coupling using soil moisture from the Global Land Data Assimilation System and observational precipitation. *Journal of Geophysical Research: Atmospheres, 113*

Zreda, M., Shuttleworth, W., Zeng, X., Zweck, C., Desilets, D., Franz, T., & Rosolem, R. (2012). COSMOS: the cosmic-ray soil moisture observing system. *Hydrology and Earth System Sciences, 16*, 4079-4099

Figures

Figure 1: Location of the Baldry study area in the central-west of NSW Australia, along with a photograph of the study area.
Figure 2: (a) Scatter plot of average daily soil moisture vs. daily evaporation; (b) scatter plot of day-to-day change in average daily soil moisture vs. day-to-day change in daily evaporation; (c) cumulative distributions of average daily soil moisture and daily evaporation; (d) cumulative distributions of day-to-day change in average daily soil moisture and daily evaporation.
Figure 3: Standardized soil moisture (COSMOS and TDR), evaporation (modelled and observed) and precipitation signatures for entire duration of record.
Figure 4: Quantile-Quantile (Q-Q) plots of standardized COSMOS soil moisture vs. standardized evaporation estimates and observations (at EC tower) for entire period of record.
Figure 5: ANOVA boxplots of standardized COSMOS soil moisture, and standardized evaporation estimates and observations for the entire time series.
Figure 6: Q-Q plots of standardized soil moisture vs. standardized evaporation for each defined period of analysis. R-values denote Pearson's correlation between standardized soil moisture and modelled evaporation for that particular period.
Figure 7: ANOVA boxplots of standardized COSMOS soil moisture, and standardized evaporation estimates and observations for each defined period of analysis.

Hydrol. Earth Syst. Sci. Discuss., doi:10.5194/hess-2016-186, 2016
Manuscript under review for journal Hydrol. Earth Syst. Sci.
Published: 17 May 2016

Hydrology and Earth System Sciences
Open Access
Discussions

Figure 8: Q-Q plots of standardized soil moisture vs. standardized evaporation for each season. R-values denote Pearson's correlation between standardized soil moisture and modelled evaporation for that particular season.

Figure 1: Location of the Baldry study area in the central-west of NSW Australia, along with a photograph of the study area.

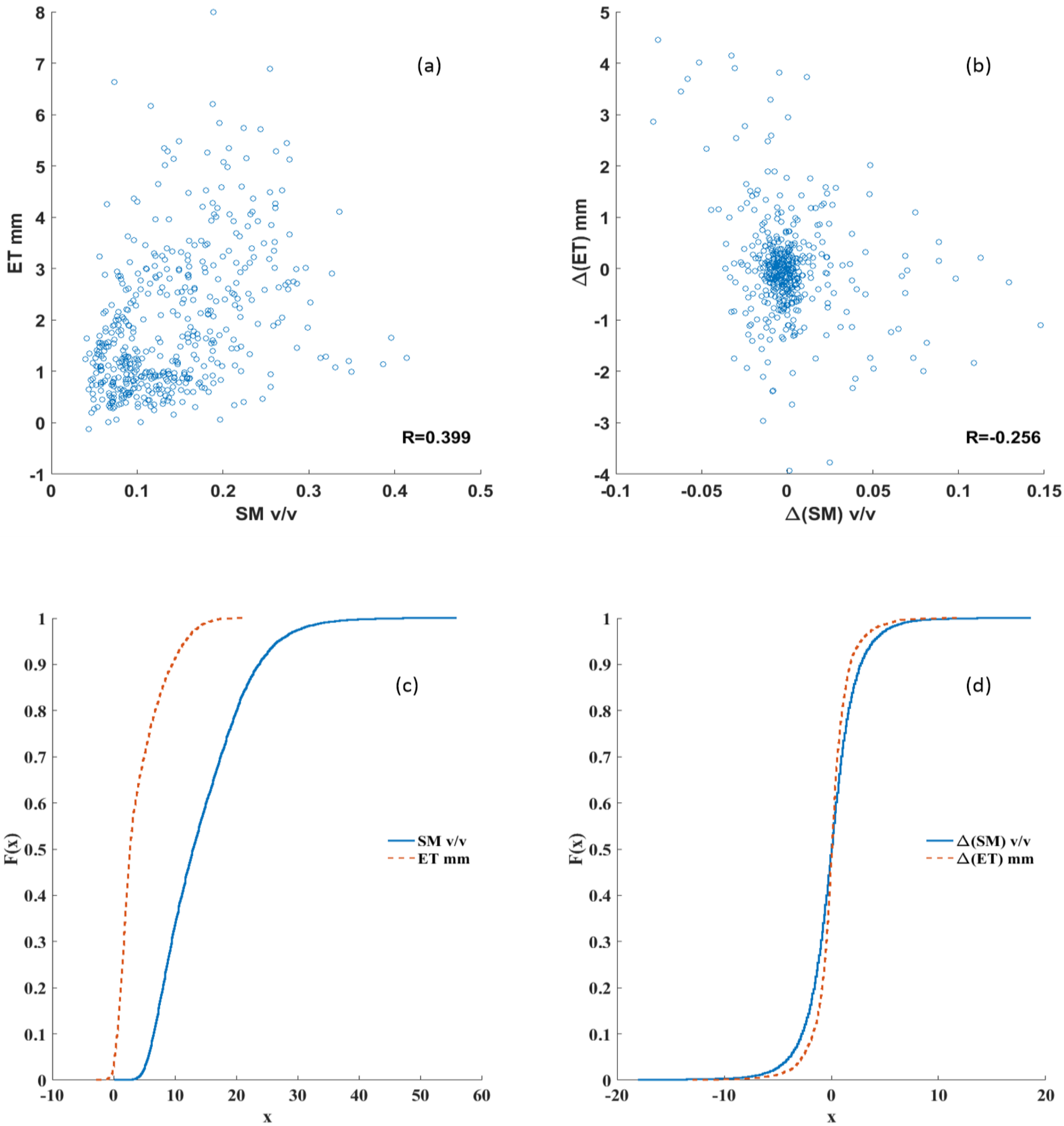

Figure 2: (a) Scatter plot of average daily soil moisture vs. daily evaporation; (b) scatter plot of day-to-day change in average daily soil moisture vs. day-to-day change in daily evaporation; (c) cumulative distributions of average daily soil moisture and daily evaporation; (d) cumulative distributions of day-to-day change in average daily soil moisture and daily evaporation.

Hydrol. Earth Syst. Sci. Discuss., doi:10.5194/hess-2016-186, 2016
Manuscript under review for journal Hydrol. Earth Syst. Sci.
Published: 17 May 2016

Hydrology and Earth System Sciences
Discussions

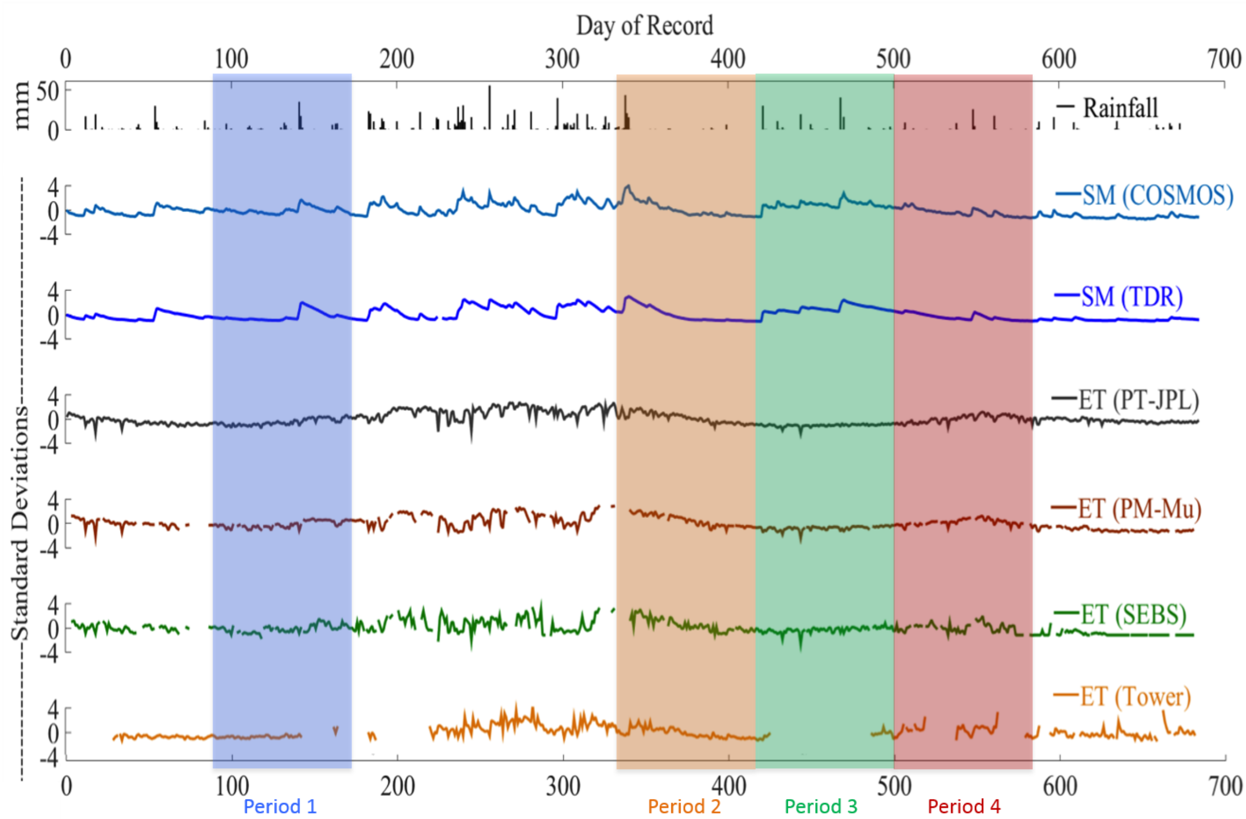

Figure 3: Standardized soil moisture (COSMOS and TDR), evaporation (modelled and observed) and precipitation signatures for entire duration of record.

Hydrol. Earth Syst. Sci. Discuss., doi:10.5194/hess-2016-186, 2016
Manuscript under review for journal Hydrol. Earth Syst. Sci.
Published: 17 May 2016

Hydrology and Earth System Sciences
Discussions
Open Access

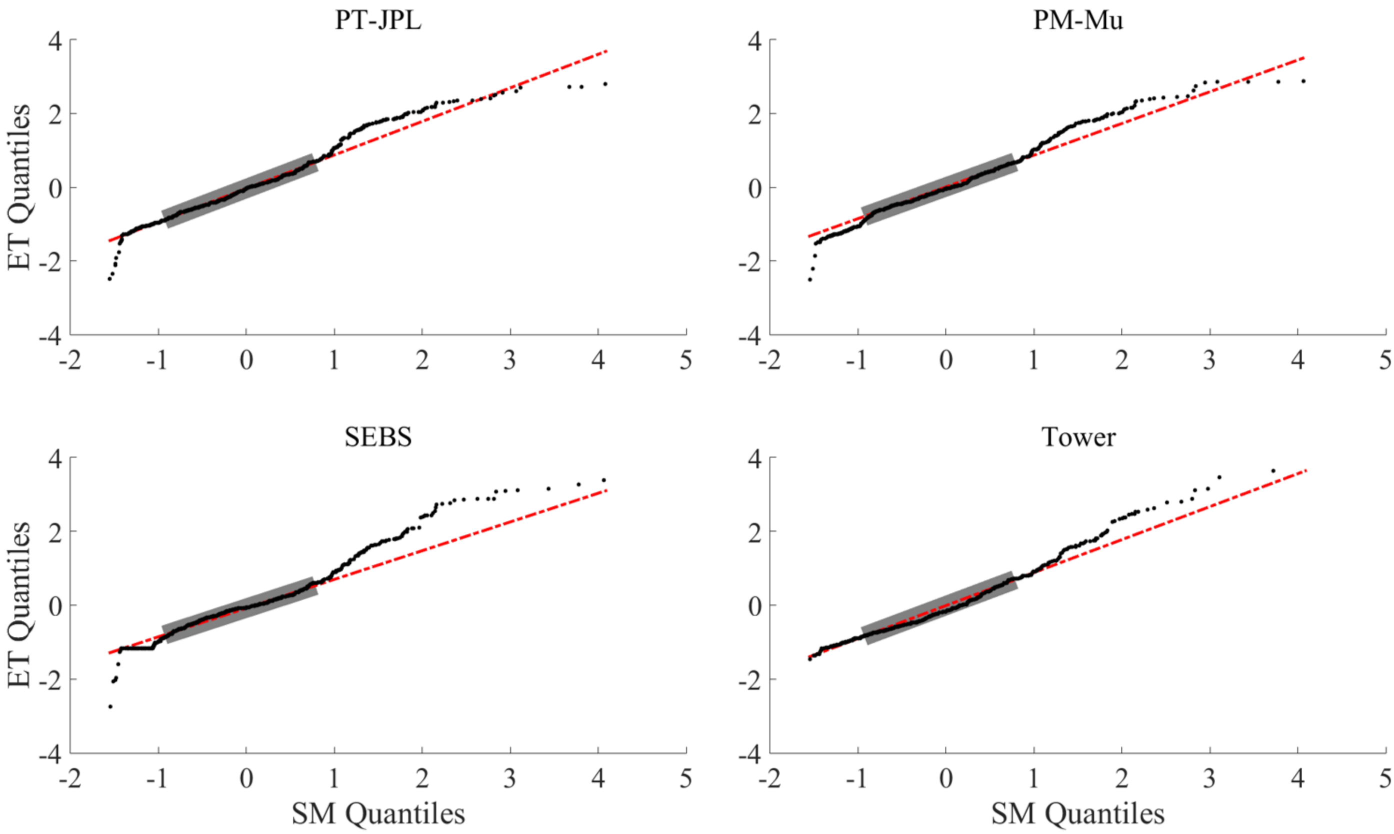

Figure 4: Quantile-Quantile (Q-Q) plots of standardized COSMOS soil moisture vs. standardized evaporation estimates and observations (at EC tower) for entire period of record.

Hydrol. Earth Syst. Sci. Discuss., doi:10.5194/hess-2016-186, 2016
Manuscript under review for journal Hydrol. Earth Syst. Sci.
Published: 17 May 2016

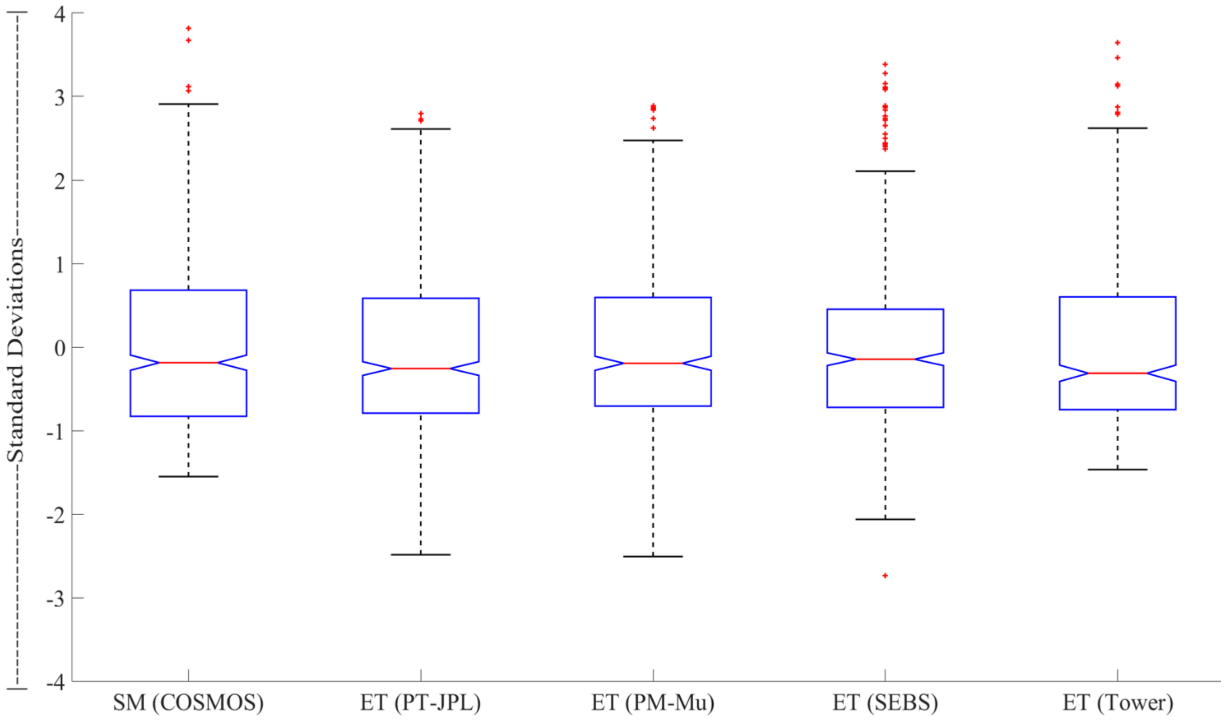

Figure 5: ANOVA boxplots of standardized COSMOS soil moisture, and standardized evaporation estimates and observations for the entire time series.

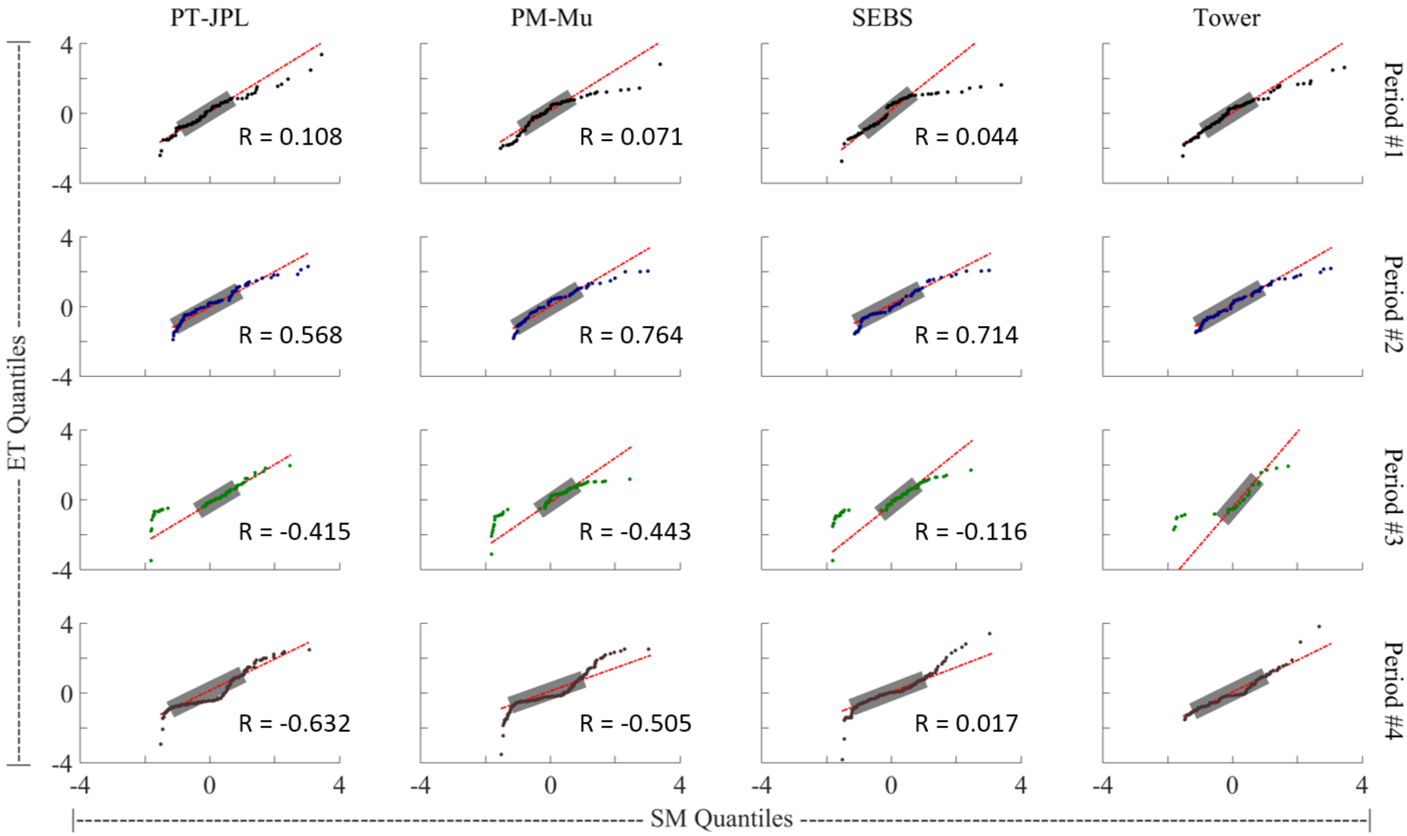

Figure 6: Q-Q plots of standardized soil moisture vs. standardized evaporation for each defined period of analysis. R-values denote Pearson's correlation between standardized soil moisture and modelled evaporation for that particular period.

Hydrol. Earth Syst. Sci. Discuss., doi:10.5194/hess-2016-186, 2016
Manuscript under review for journal Hydrol. Earth Syst. Sci.
Published: 17 May 2016

Hydrology and Earth System Sciences
Open Access
Discussions

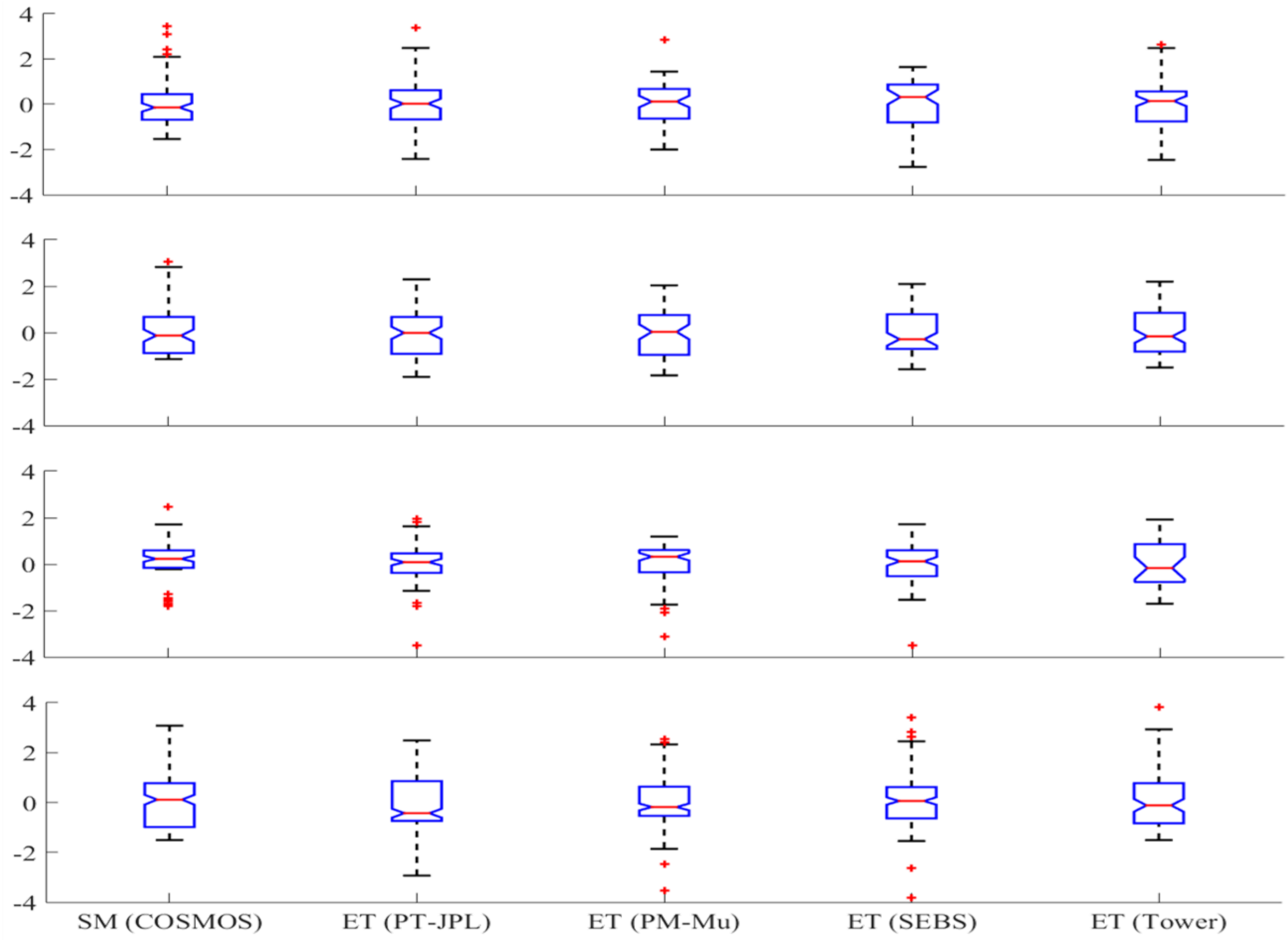

Figure 7: ANOVA boxplots of standardized COSMOS soil moisture, and standardized evaporation estimates and observations for each defined period of analysis.

Hydrol. Earth Syst. Sci. Discuss., doi:10.5194/hess-2016-186, 2016
Manuscript under review for journal Hydrol. Earth Syst. Sci.
Published: 17 May 2016

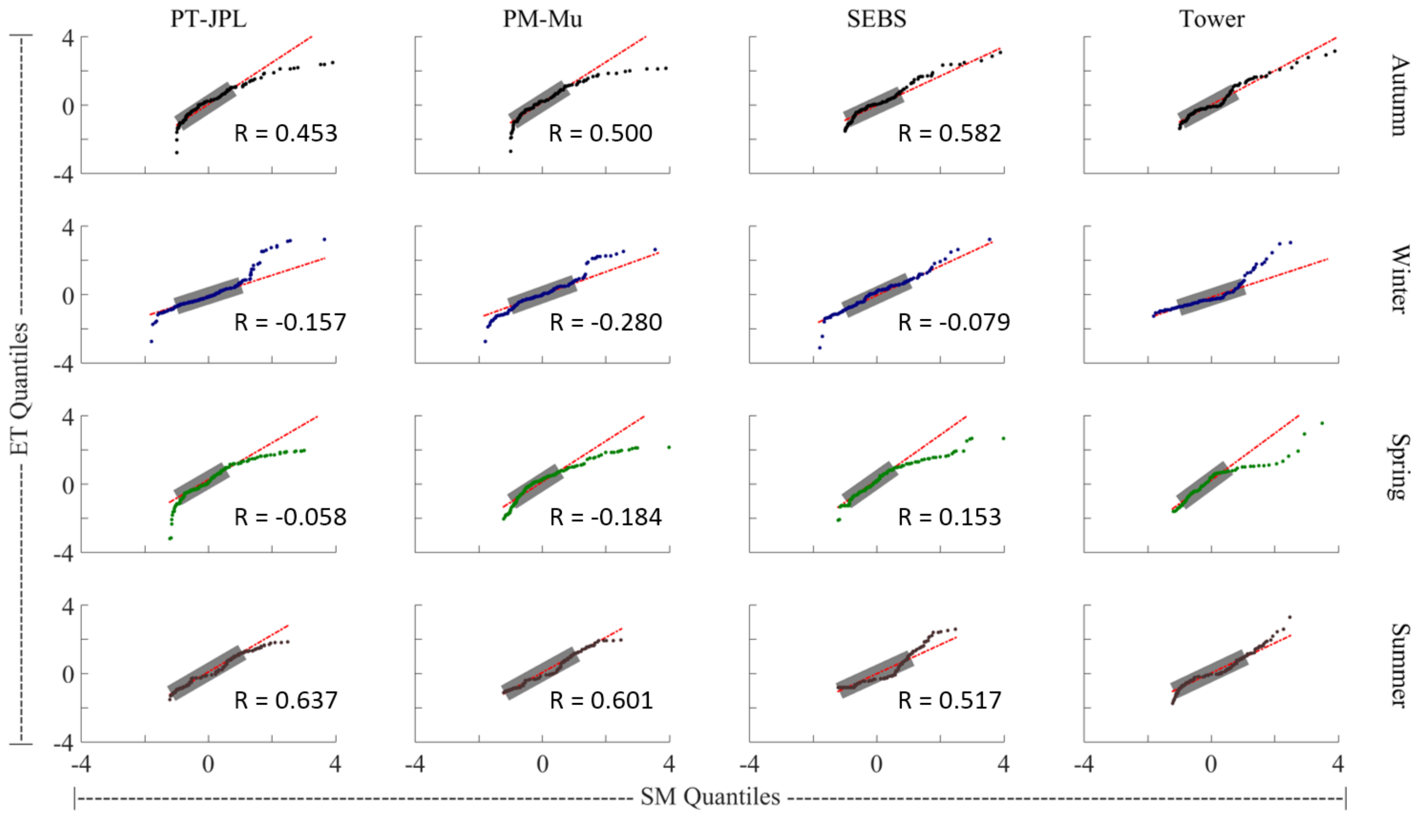

Figure 8: Q-Q plots of standardized soil moisture vs. standardized evaporation for each season. R-values denote Pearson's correlation between standardized soil moisture and modelled evaporation for that particular season.